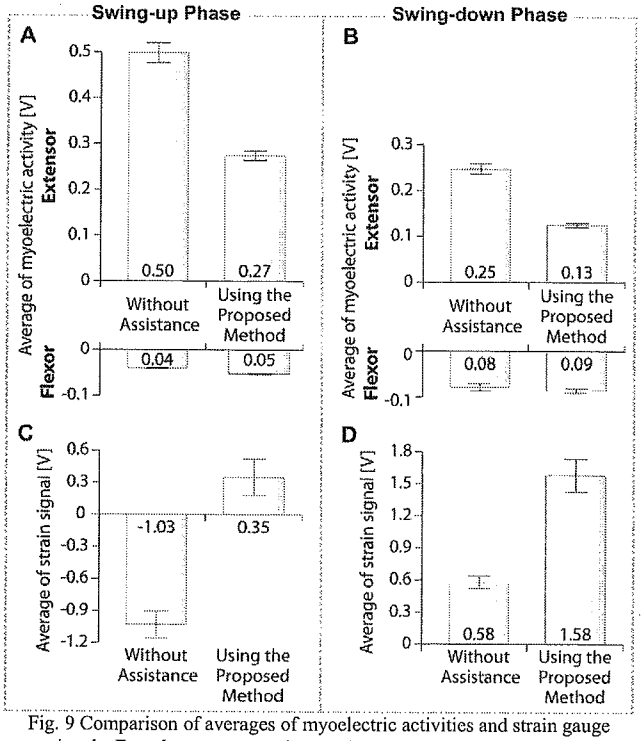

Fig. 9 Comparison of averages of myoelectric activities and strain gauge signals. Error bars represent the standard deviation of mean values.

although we compensated the mechanical impedance of HAL. It is very hard to completely compensate the mechanical impedance of practical exoskeleton-actuator system, because of an error of model parameters, a delay in control and so on.

When the proposed method was applied, HAL extended operator's knee joint in swing-up phases and acted on operator's knee joint in the extending direction in swing-down phases. These workings of HAL are fitting to major roles of operator's muscles in each phase. Additionally, reductions of operator's myoelectric activities were observed. Therefore, We consider that HAL has acted as muscles instead of operator's muscles appropriately by using the proposed method to control actuators of HAL.

However, when the proposed method was applied, the myoelectric activities of the flexor increased as compared to the case without any assisting method. This result implies also that the operator produced the muscle torque to flex the knee joint because HAL has restrained knee flexion more than the operator has expected. We consider that the gain parameter α_ζ =0.5 is still too large in this experiment. It will be necessary to develop a method to adjust the gain parameters appropriately as a future work.

VI. Conclusion

We have proposed the method to control actuators of HAL by referring to Biological and Motion Information to use the robot suit as operator's muscles. In this method, HAL produces torque corresponding to muscle contraction torque by referring to the myoelectricity that is the biological information to control operator's muscles. In addition, operator's viscoelasticities are estimated from motion information using an on-line parameter identification method. The model of operator's lower limb equipped with HAL was constructed in order to estimate operator's viscoelastic properties. The viscoelasticity of the actuator of HAL was adjusted to be proportional to operator's viscoelasticity by using the impedance control method.

To evaluate the effectiveness of the proposed method, the method was applied to a swinging motion of operator's lower leg. The experimental results suggested that the proposed method is useful to use HAL as operator's muscles. As a result of this experiment, we have confirmed the effectiveness of the proposed method.

Acknowledgment

This study was partially supported by the Ministry of Education, Culture, Sports, Science and Technology of Japan, Grant-in-Aid for Scientific Research (A).

References

[1] Okamura J., Tanaka H. and Sankai Y. EMG-based Prototype Powered Assistive system for Walking Aid. In Proc. Asian Symposium on Industrial Automation and Robotics (ASIAR'99), Bangkok, Thailand, pp.229-234, (1999).

[2] Nakai T., Lee S., Kawamoto H. and Sankai Y. Development of Power Assistive Leg for Walking Aid using EMG and Linux. In Proc. The 2nd Asian Conference on Industrial Automation Robotics (ASIAR2001), Bangkok, Thailand, pp.295-299, (2001).

[3] Kawamoto H. and Sankai Y. Power Assist System HAL-3 for Gait Disorder Person. In Proc. of International Conference on Computers Helping People with Special Needs (ICCHP 2002), Linz Austria, pp.196-203, (2002).

[4] Gordon K.E. and Ferris D.P. Proportional myoelectric control of a virtual object to investigate human efferent control. Experimental Brain Research, 159, pp.478-486.

[5] Winter D.A., Patla, A.E., Francois F., Ishac M. and Gielo-Perczak K. Stiffness Control of Balance in Quiet Standing. Journal of Neurophysiology 80, pp. 1211-1221, (1998).

[6] Gomi H. and Osu R. Task-Dependent Viscoelasticity of Human Multijoint Arm and Its Spatial Characteristics for Interaction with Environments. J Neurosci, 18, pp. 8965-78 (1998).

[7] Lee S. and Sankai Y. Power Assist Control for Walking Aid with HAL-3 Based on EMG and Impedance Adjustment around Knee Joint. In Proc. of IEEE/RSJ International Conf on Intelligent Robots and Systems (IROS 2002), EPFL, Switzerland, pp.1499-1504, (2002).

[8] Lee S. and Sankai Y. Power assist control for leg with hal-3 based on virtual torque and impedance adjustment. In Proc. IEEE International Conference on Systems, Man and Cybernetics (SMC), Hammamet, Tunisia, TP1B3 (CD-ROM), (2002).

[9] Lee S. and Sankai Y. The Natural Frequency-Based Power Assist Control for Lower Body with HAL-3. In Proc. of IEEE International Conference on System, Man and Cybernetics (SMC), Washington USA, (2003).

[10]Cavanagh, P.R., Komi, P.V. Electromechanical Delay in Human Skeletal Muscle under Concentric and Eccentric Contractions. European Journal of Applied Physiology, 42, 159-163 (1979).

[11]Park, E. and Meek, S.G. Fatigue compensation of the electromyographic signal for prosthetic control and force estimation. IEEE Transactions on Biomedical Engineering, vol. 40, Oct. (1993).

日本機械学会論文集(C編)
71巻705号(2005-5)

論文 No. 04-0420

装着型下肢用パワーアシストシステムによる振り運動での仮想インピーダンス調整に関する研究*

李 秀雄*1, 山海嘉之*2

Minimizing the Physical Stress by Virtual Impedance of Exoskeletal Robot in Swinging Motion with Power Assist System for Lower Limb

Suwoong LEE*3 and Yoshiyuki SANKAI

*3 Intelligent Systems Institute, National Institute of Advanced Industrial Science and Technology,
Graduate School of Systems and Information Engineering, University of Tsukuba,
1-1-1 Umezono, Tsukuba-shi, Ibaraki, 305-8568 Japan

The objective in this paper is to suggest the method to examine the relationship between impedance of exoskeletal robot and physical stress of the operator in order to minimize the operator's physical stress in swinging motion. The exoskeletal robot, "HAL-3" which we developed for assisting the motor function of lower limb was used for experiments in this research. To accomplish the objective, first, the physical parameters around joint of HAL-3 were identified, secondly, the relationships between virtual impedance values and physical stress of operator were examined through experiments for swinging motions. The physical stress was evaluated with myoelectricity, joint torque, and operator's feelings during the experimental motion. As the results, we found the physical stress tended to decline with the decrease of virtual inertia and coulomb friction, and to increase slightly with the decrease of gravitational torque. The decrease of virtual viscous friction coefficient made the physical stress increase gradually after it declined to trough at the positive virtual viscous friction. We could establish the criteria to adjust the virtual impedances for minimizing the operator's physical stress in swinging motion based on these examined results.

Key Words: virtual impedance, physical stress, HAL-3, parameter identification, swinging motion

1. はじめに

工場での作業支援や高齢者の動作補助等を目的とした装着型の外骨格パワーアシストシステムは，人間の運動を補助する上で望ましい形態を持っていると考えられ，今後，製造業等の労働集約的な産業や医療-福祉分野等で大いに活躍すると期待されている(1)~(3).

外骨格パワーアシストシステムが人間と協調し，効率よく運動を補助する為には，力やトルクの増幅だけではなく，系全体の安定性や操作性の向上を考慮した機械インピーダンスの適切な設定が必要である．これに関連した従来の研究では，ランダムな目標入力に対するロボットと人間の機械インピーダンス変化(5)や，位置決め作業におけるロボットの仮想機械インピーダンス調整法(6)等，主に与えられた目標値に従って運動した時のロボットと人間のインピーダンス特性を扱っていた．しかし，人間の運動は常に随意的とは限らず，図1に示した脚や腕の振り運動のように，不随意的で反復的な場合もあり，これらは日常で起こりうる動作の中でも頻繁に実施される．従って，外骨格パワーアシストシステムによって装着者の様々な運動を円滑に補助する為には，不随意的な振り運動におけるインピーダンス特性も考慮しなくてはならない．しかし，パワーアシストシステムに関連して，上肢や下肢の振り運動における機械インピーダンス特性を解析した研究は未だ行われていない．上肢や下肢の振り運動では床面等の外部環境から拘束が無く，慣性モーメントや重力が巧みに利用され，非常に小さな力により実行される(8)．従って，外骨格型パワーアシストシステムを用いて振り運動を効率よく補助する為には，外骨格の慣性モーメントや粘性摩擦等の各インピーダンスが運動に及ぼす影響を解析し，この解析を基に各インピーダンスの調整基準を設ける必要がある．そこで本論文では，下肢用外骨格パワーアシストシステムを用いた実験により，外骨格のインピーダンスによる負荷を最小にし，振り運動を効率的に実現する為には仮想インピーダンスがどのように調整されるべきかという基準の設定方法を提案する．

* 原稿受付 2004年4月12日.
*1 正員，産業技術総合研究所知能システム研究部門(〒305-8568 つくば市梅園1-1-1).
*2 筑波大学大学院システム情報工学研究科.
E-mail: lee-sirg@aist.go.jp

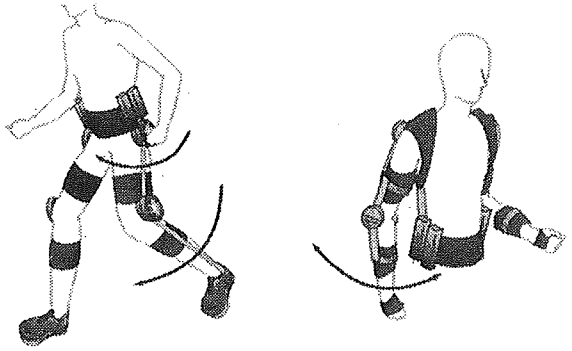

Fig. 1　Operators Putting on Exoskeletal Robots in Swinging Motion

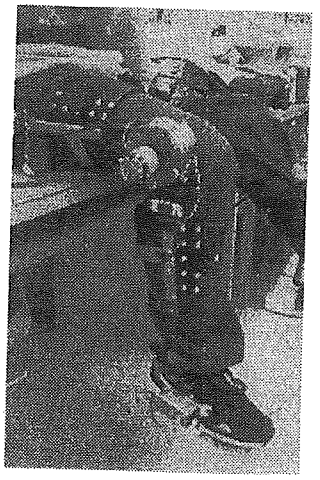

Fig. 2　Exoskeletal structure of HAL-3

2. HAL (Hybrid Assistive Limb) -3

2·1 HAL-3 のハードウェア構成　本研究で行われる実験には，下肢運動機能補助用装着型パワーアシストシステム HAL (Hybrid Assistive Limb) -3 を用いた[9]~[11]．図 2 に HAL-3 を装着した被験者を示す．

HAL-3 には，装着者の運動に関する情報を計測する為の各種センサが備えられている．今回の実験では独自に開発した表面筋電位センサにより装着者の膝関節伸筋（大腿直筋）と屈筋（大腿二頭筋）の二箇所の筋活動を，外骨格の膝関節内側に設置されたポテンショメータにより膝関節の動作角度を計測した．また下腿部を固定するフレームに設けられた力センサにより，外骨格に作用する装着者の力を計測した．これらのセンサから計測されたデータは計測・制御用小型コンピュータに取り込まれ処理される．

DC サーボモータとギアによって構成されるアクチュエータは，計測・制御用コンピュータから算出された指令信号に従ってトルク制御で駆動される．また，アクチュエータは外骨格の各関節中心を基準としてフレームに取り付けられており，これによって，関節回りの運動における慣性モーメントの影響を最小化している．膝関節以下下腿部の外骨格フレームは被験者によって 0.47[m]~0.5[m] の範囲で長さを調整した．

2·2 逐次最小自乗法を用いた下腿部外骨格系のパラメータ同定　本研究では予備実験として，仮想インピーダンス調整の基本となる外骨格系の慣性モーメント，粘性摩擦等の動力学パラメータを逐次最小二乗法を用いて同定した[11][13]．先ず，膝関節回りの外骨格系を式 (1) のように表す．

$$I_h\frac{d^2\theta(t)}{dt^2}+D_h\frac{d\theta(t)}{dt}+M_hgl_hsin\theta(t)+C_asign\left(\frac{d\theta(t)}{dt}\right)=\tau_a(t) \quad (1)$$

ここで I_h，D_h，M_h，C_a はそれぞれ外骨格系膝関節回りの慣性モーメント，粘性摩擦係数，質量，クーロン摩擦である．また g は重力加速度，l_h は外骨格の関節中心から重心までの距離，$\theta(t)$ は鉛直方向を基準とした角度，$sign\left(\frac{d\theta(t)}{dt}\right)$ は角速度の符号，$\tau_a(t)$ はアクチュエータにより発生されるトルクである．パラメータ同定アルゴリズムを適用する為に，式 (1) を式 (2) のようにまとめる．

$$\Omega(t)X=\tau_a(t) \quad (2)$$

ここで

$$\Omega(t)=\left[\frac{d^2\theta(t)}{dt^2}\ \frac{d\theta(t)}{dt}\ sin\theta(t)\ sign\left(\frac{d\theta(t)}{dt}\right)\right] \quad (3)$$

$$X=[I_h\ D_h\ M_hgl_h\ C_a]^T \quad (4)$$

同定するパラメータと計測トルク-推定トルクの誤差をそれぞれ $\hat{X}(t)$ と ε と定義した場合，アクチュエータのトルク $\tau_a(t)$ は式 (5) のように示すことが出来る．

$$\tau_a(t)=\Omega(t)\hat{X}(t)+\varepsilon=\hat{\tau}_a(t)+\varepsilon \quad (5)$$

従って，式 (5) に基づいた二次の評価関数 $J(t)$ を最小にする条件

$$J(t)=\varepsilon^2=\left(\tau_a(t)-\Omega(t)\hat{X}(t)\right)^2 \quad (6)$$

$$\frac{\partial J(t)}{\partial\hat{X}(t)}=0 \quad (7)$$

からパラメータは式 (8) のように算出される．

$$\hat{X}(t)=\left(\Omega(t)^T\Omega(t)\right)^{-1}\left(\Omega(t)^T\tau_a(t)\right) \quad (8)$$

角速度，角加速度データは角度信号を平滑化微分して算出し，トルクデータは計測された駆動電流から求めた．同定実験時に採用したアクチュエータのトルクパ

Table 1　Identified parameters of exoskeleton

Parameter	Identified value	S.D.
Inertia moment [kg·m^2]	0.17	±0.001
Viscous coeff. [N·m/(rad/sec)]	3.13	± 0.08
Gravitational toque [N·m]	3.31	± 0.004
Coulomb friction [N·m]	0.57	± 0.02

ターンは同定演算の精度や実験時の伝達系の振動を考慮して，周波数 0.33，0.67，1.33[Hz] の正弦波とした．実験回数は 10 回とし，パラメータ同定の結果は平均値によって決定する．求められた各インピーダンスを表 1 に示す．

3. 実　　験

本研究では，下腿部の振り運動による実験を通じて 1）仮想慣性モーメント，仮想粘性摩擦等の各仮想インピーダンスを個々に変化させた場合と，2）1）の実験結果に基づいて，全 4 種類の仮想インピーダンスを適切な値に調整した場合における負荷の変化を解析した．

3·1　実験方法

3·1·1　装着者と HAL による人間-ロボット系の構成

HAL-3 の外骨格系を含んだ装着者の下腿部は式 (9) のように表すことが出来る．

$$(I_s+I_h)\frac{d^2\theta(t)}{dt^2}+(D_s(u(t))+D_h)\frac{d\theta(t)}{dt}+(M_sl_s+M_hl_h)\,g\sin\theta(t)+C_a sgn\left(\frac{d\theta(t)}{dt}\right)=\tau_a(t)+\tau_m(t)\quad(9)$$

但し I_s，D_s，M_s，l_s はそれぞれ装着者の膝関節回りの慣性モーメント，粘性摩擦係数，質量，関節から重心までの距離である．$u(t)$ は筋の活性度，$\tau_m(t)$ は装着者の筋によって発生されるトルクである．式 (9) で外骨格の動力学パラメータ I_h，D_h，M_hgl_h および C_a は Table.1 の値であり，装着者の膝関節筋骨格系回りの弾性は無視する．補償する慣性モーメント，粘性摩擦係数，重力モーメント，クーロン摩擦をそれぞれ I_h-I_v，D_h-D_v，$(M_h-M_v)gl_h$，C_a-C_v とし，アクチュエータにより式 (10) の様な補償トルク

$$\tau_a(t)=(I_h-I_v)\frac{d^2\theta(t)}{dt^2}+(D_h-D_v)\frac{d\theta(t)}{dt}+(M_h-M_v)\,gl_h\sin\theta+(C_a-C_v)\,sgn\left(\frac{d\theta(t)}{dt}\right)\quad(10)$$

Table 2　Setting condition of virtual impedance

Virtual impedance	Set value	Tolerance
I_v[kg·m^2]	0.170 ~ -0.020	-0.020
D_v[N·m/(rad/sec)]	3.128 ~ -0.782	-0.391
M_hgl_h[N·m]	3.310 ~ -0.828	-0.414
C_v[N·m]	0.560 ~ -0.140	-0.070

を発生させた場合，式 (11)

$$(I_s+I_v)\frac{d^2\theta(t)}{dt^2}+(D_s(u(t))+D_v)\frac{d\theta(t)}{dt}+(M_sl_s+M_vl_h)\,g\sin\theta+C_v sgn\left(\frac{d\theta(t)}{dt}\right)=\tau_m(t)\quad(11)$$

のように実験中の動作は行われる．ここで I_v，D_v，M_vgl_h および C_v はそれぞれ任意に設定可能な仮想インピーダンスである．

図 3 に実験系全体の構成を示す．先ず，長時間の実験による負担を掛けず安定に下腿部の振り運動を行わせる為に，装着者を一定の高さ以上の頑丈な台に着席させた．実験中の角度と表面筋電位の計測は 1[msec] の周期で，アクチュエータによる補償トルクの制御は 5[msec] の周期で行われた．表面筋電位は計測前に 2 次のアナログローパスフィルタ（カットオフ周波数：500[Hz]）・を用いて処理されている．計測されたデータは HAL-3 側の計測・制御用コンピュータに保存されると共に，実験者側のコンピュータを通じてリアルタイムでモニタリングされる．

3·1·2　実験条件の設定

実験動作として行う振り運動を，異なる種類，変化の仮想インピーダンスに対して評価する為に，同一の角度目標値，周波数に従って行った．但し，角度目標値の設定は，正確な位置決め動作を行う事を目的としてない事に注意する．今回の実験では角度目標値を ±0.5[rad]，運動周波数は 1[Hz] と設定した [8] [12]．図 4 に実験中に計測された屈筋・伸筋での表面筋電位の絶対値（この図では伸筋における表面筋電位を負で示す），力センサの情報から算出された負荷トルク，および角度データを示す．

実験は，2 種類に分けて行われた．先ず基礎実験として，表 2 のように各仮想インピーダンスを 10 段階で調整し，振り動作を行った．この時，1 回の動作における試行時間は 10 秒とした．一連の調整が終わったところで 1 セットとし，各仮想インピーダンスに対して 5 セット動作実験を行った．次に応用実験として，基礎実験結果に基づき，4 種類の仮想インピーダンスをそれぞれ適切に調整し，同一動作により実験を行った．この実験のインピーダンス設定条件等は基礎実験

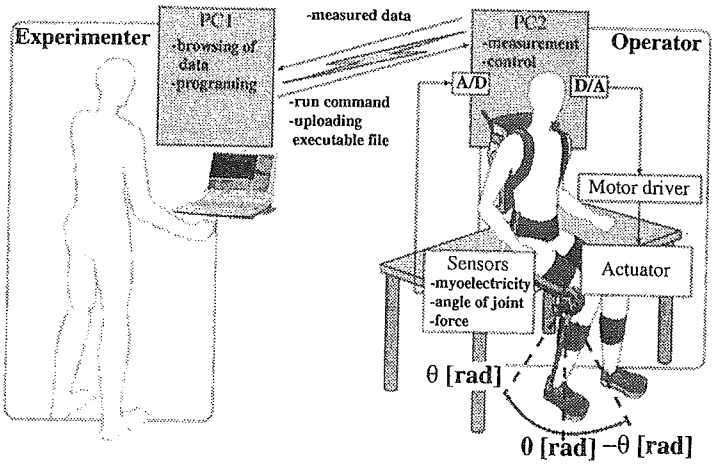

Fig. 3　Experimental setup

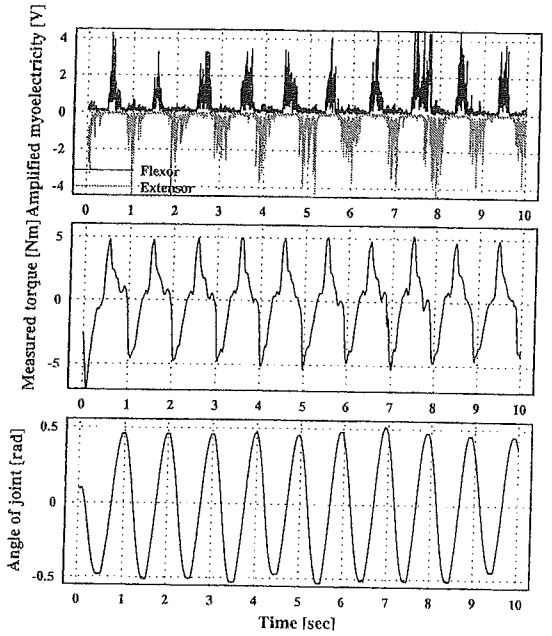

Fig. 4　Data of experimental motion

結果によって構成する．なお，各セットの間には十分な休憩時間を挟んで実験を行い，疲労の影響が表面筋電位や装着者の運動に表れないように配慮した．被験者は20代の健常な成人男性3人とした．

3·1·3　実験動作の評価　運動の評価指標は力センサを基に算出された負荷トルクの平均値

$$J_{\tau_m}(i)=\frac{1}{t_f}\int_0^{t_f}|\tau_m(t,i)|dt \tag{12}$$

と膝関節伸筋（内側広筋）と屈筋（大腿二頭筋）での表面筋電位の積分値を実験中の最大値で正規化した値，

$$J_{m_f}(i)=J_f(i)/J_{f_{max}} \tag{13}$$

$$J_{m_e}(i)=J_e(i)/J_{e_{max}} \tag{14}$$

$$J_f(i)=\int_0^{t_f}|m_f(t,i)|dt \tag{15}$$

$$J_e(i)=\int_0^{t_f}|m_e(t,i)|dt \tag{16}$$

$$J_{f_{max}}=max\{J_f(1),\cdots,J_f(n)\} \tag{17}$$

$$J_{e_{max}}=max\{J_e(1),\cdots,J_e(n)\} \tag{18}$$

および運動終了後の主観的な評価として，操作感および抵抗感を用いる．ここでnは一人の被験者に対する実験の全試行回数，t_fは試行時間，$\tau_m(t,i)$は負荷トルクの計測値，$J_{\tau_m}(i)$は負荷トルクの平均値，$m_f(t,i)$，$m_e(t,i)$，$J_{m_f}(i)$，$J_{m_e}(i)$はそれぞれ伸筋・屈筋の表面筋電位およびその正規化した値，$J_f(i)$，$J_e(i)$，$J_{f_{max}}$，$J_{e_{max}}$はそれぞれ伸筋・屈筋の表面筋電位の積分値およびそのn個データ中の最大値である．主観による評価は表3のように，操作感と抵抗感それぞれの項目に対して7段階で行った[6][14][15]．ここで操作感は「意図通りに脚を振る事が出来る」といった感覚，また抵抗感は動作における「軽い」あるいは「重い」といった感覚と定義した．各被験者がこれらの感覚を十分理解出来るように，実験開始前に数回リハーサルを行った．主観による評価の尺度として，外骨格からアクチュエータを取り外し，関節回りの慣性モーメントおよび摩擦が極めて少ない状態で運動を行った場合の操作感と抵抗感の値をそれぞれ0に，アクチュエータを取り付け仮想インピーダンスが調整されていない状態で運動を行った場合の操作感と抵抗感をそれぞれ2と-3に設定した．

運動評価は主に負荷トルクと主観による評価によって行い，表面筋電位は伸屈筋が拮抗した状態等，運動と直接関係の無い筋活動も反映される為，補助的な評価指標として用いる．

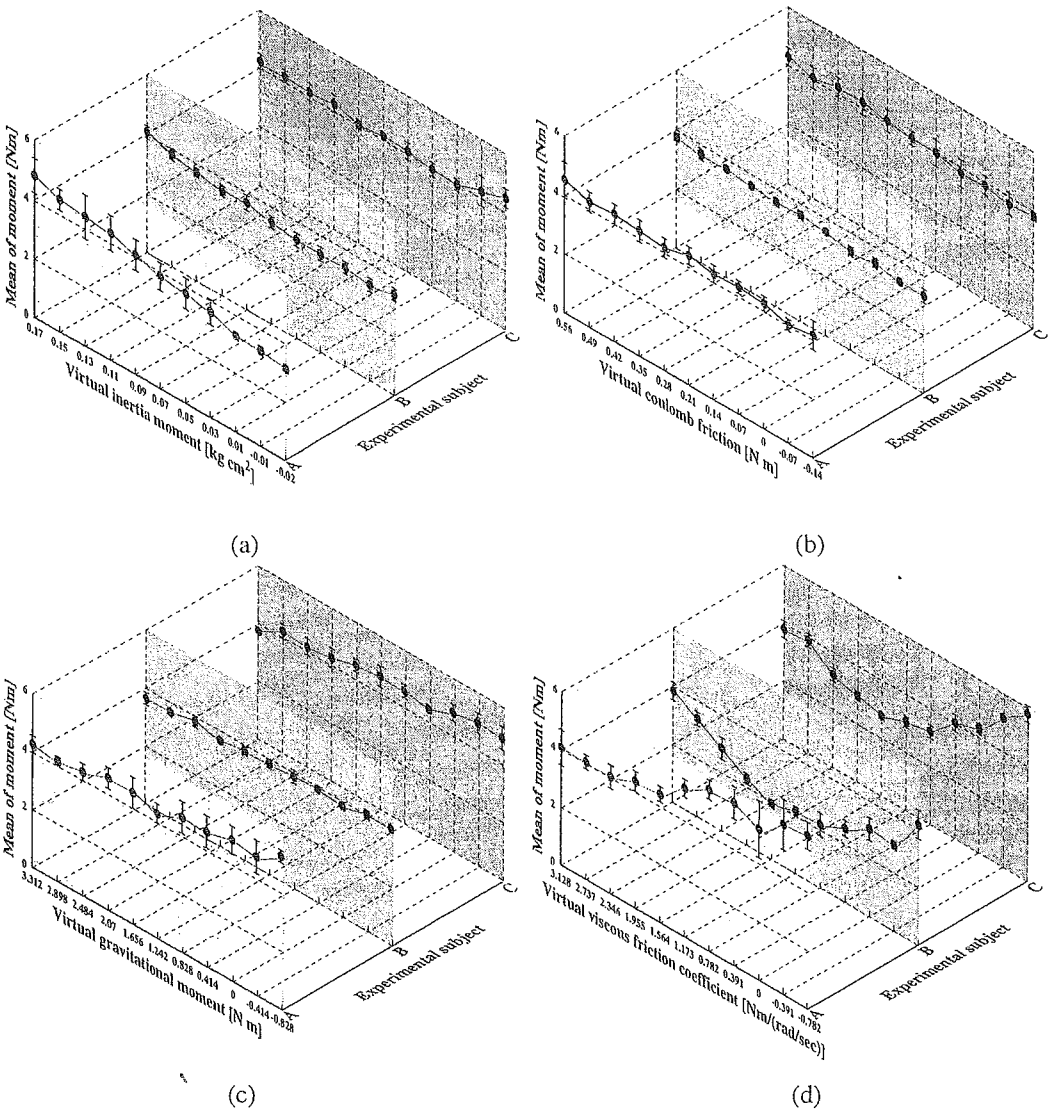

Fig. 5　Experimental results of musculoskeletal moment.

Table 3　Evaluation of operationality and stress

mark	-3	-2	-1	0	1	2	3
opera -tion	very bad	bad	little bad	-	little good	good	very good
stress level	very high	high	little high	-	little low	low	very low

3·2　実験結果

3·2·1　各インピーダンス別調整に対する運動の変化

図5，6，7に負荷トルク，屈筋の表面筋電位の平均値，伸筋の表面筋電位の平均値を示した．(a)，(b)，(c)，(d)はそれぞれ仮想慣性モーメント，仮想クーロン摩擦，仮想重力モーメント，仮想粘性摩擦係数の調整に対するデータを示す．実験データは被験者一人当たり220回，合計660回動作を実行した結果として得られたものである．仮想慣性モーメントおよび仮想クーロン摩擦では，その値が正の値である場合，これらの軽減と共に装着者への負荷トルクおよび伸筋・屈筋の表面筋電位が徐々に低下する傾向を示した．特に被験者A，Bでは負荷トルクの値にその変化が著しく表れている．これに対して仮想慣性モーメントと仮想クーロン摩擦が負の値である場合，負荷トルクが減少する傾向はほぼ一定に維持，あるいは僅かに上昇しており，外骨格の仮想インピーダンスが不安定になる事で運動の負担が徐々に増している事を示唆している．

仮想重力モーメントを補償した場合には被験者A，B，C共に負荷トルクが僅かに増加した．また表面筋電位の値は被験者によって伸屈筋共に徐々に増加する場合と僅かに増減を繰り返す場合に分かれた．このデータからは装着者が振り運動時に外骨格の質量を負荷と

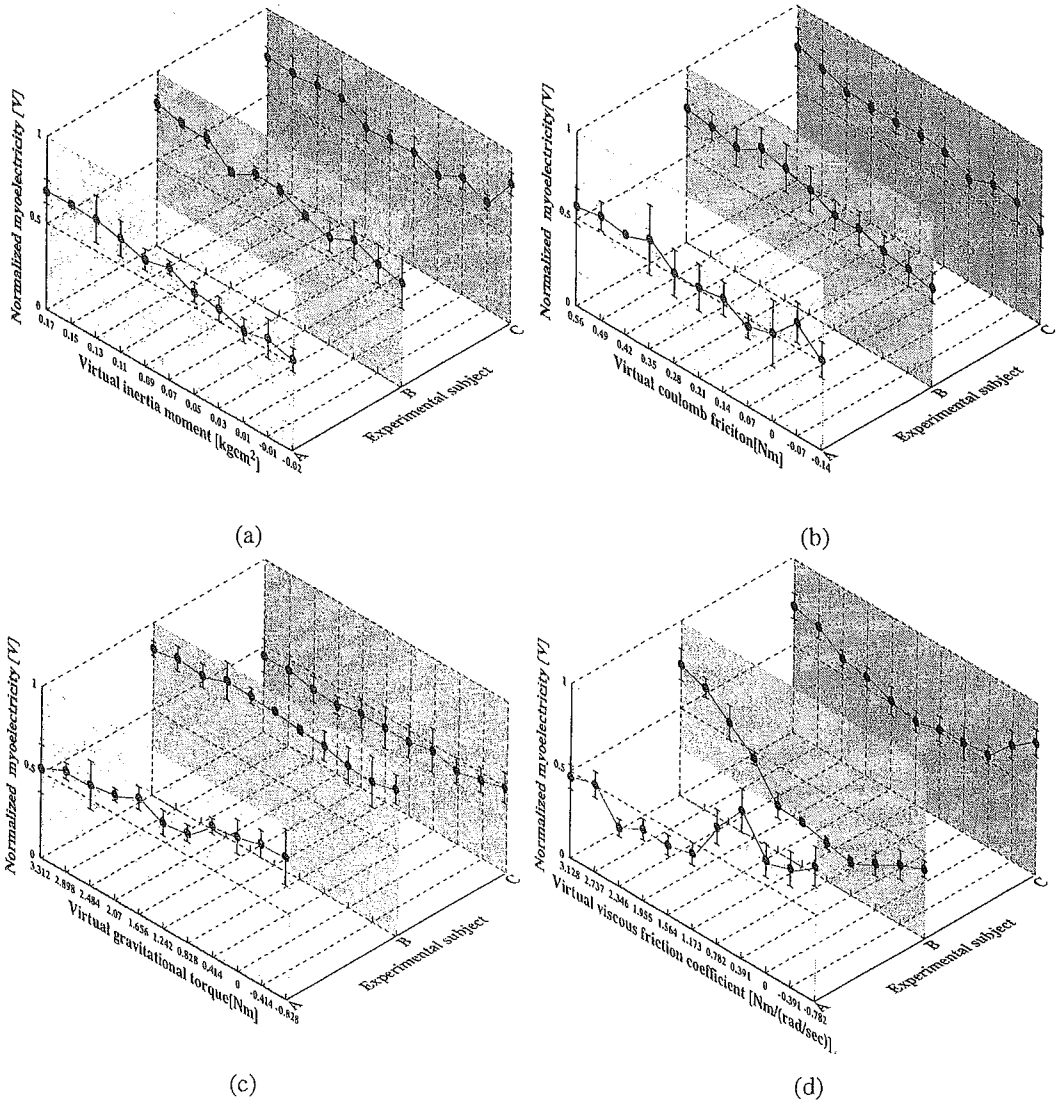

Fig. 6　Experimental results of myoelectricity at flexor muscle.

していない事が判り，質量による重力モーメントをむしろ巧みに利用する事で運動を効率よく行っている可能性が示された．

仮想粘性摩擦を調整した場合には，被験者Aと被験者B，Cで，運動データでの変化が分かれた．前者の場合，仮想粘性摩擦を補償した直後に負荷トルク，屈筋の表面筋電位共に増加しており，他被験者のデータに比べ負荷トルクの変化が不規則的で全体的にデータの上下の変化が大きい特徴を示した．これにより被験者Aは被験者B，Cに比べ，筋を積極的に使って仮想粘性摩擦の変化に対処しているが，安定かつ適切に対応出来ていないと考えられる．後者の場合では仮想粘性摩擦係数の変化と共に負荷トルクと屈筋の表面筋電位が減少していたが，仮想粘性摩擦係数が0に至る前に増加へと変化した．伸筋の表面筋電位の変化は3人の被験者共に，ある時期一定レベルを維持した後，急激に増加した．これにより3人の装着者の運動に対して，外骨格の理想的な仮想粘性摩擦は0ではない事が判明した．この原因としては軽減された仮想粘性摩擦に対して慣性モーメントが比較的大きい事とHALを装着した被験者達が粘性摩擦の変化に敏感に反応し，伸筋・屈筋により関節回りのインピーダンスを徐々に高めている事が考えられる．

3·2·2　全仮想インピーダンス調整に対する運動の変化　次に仮想慣性モーメント，仮想粘性摩擦，仮想重力モーメントおよび仮想クーロン摩擦といった全ての仮想インピーダンスを調整し実験を行った．試行回数は前述の実験と同様，一人当たり220回とした．この実験では前節の結果に基づき，仮想慣性モーメントおよび仮想クーロン摩擦は0に設定した．また装着者は外骨格の質量による重力モーメントを巧みに利用していると判断し，仮想重力モーメントの調整は行わな

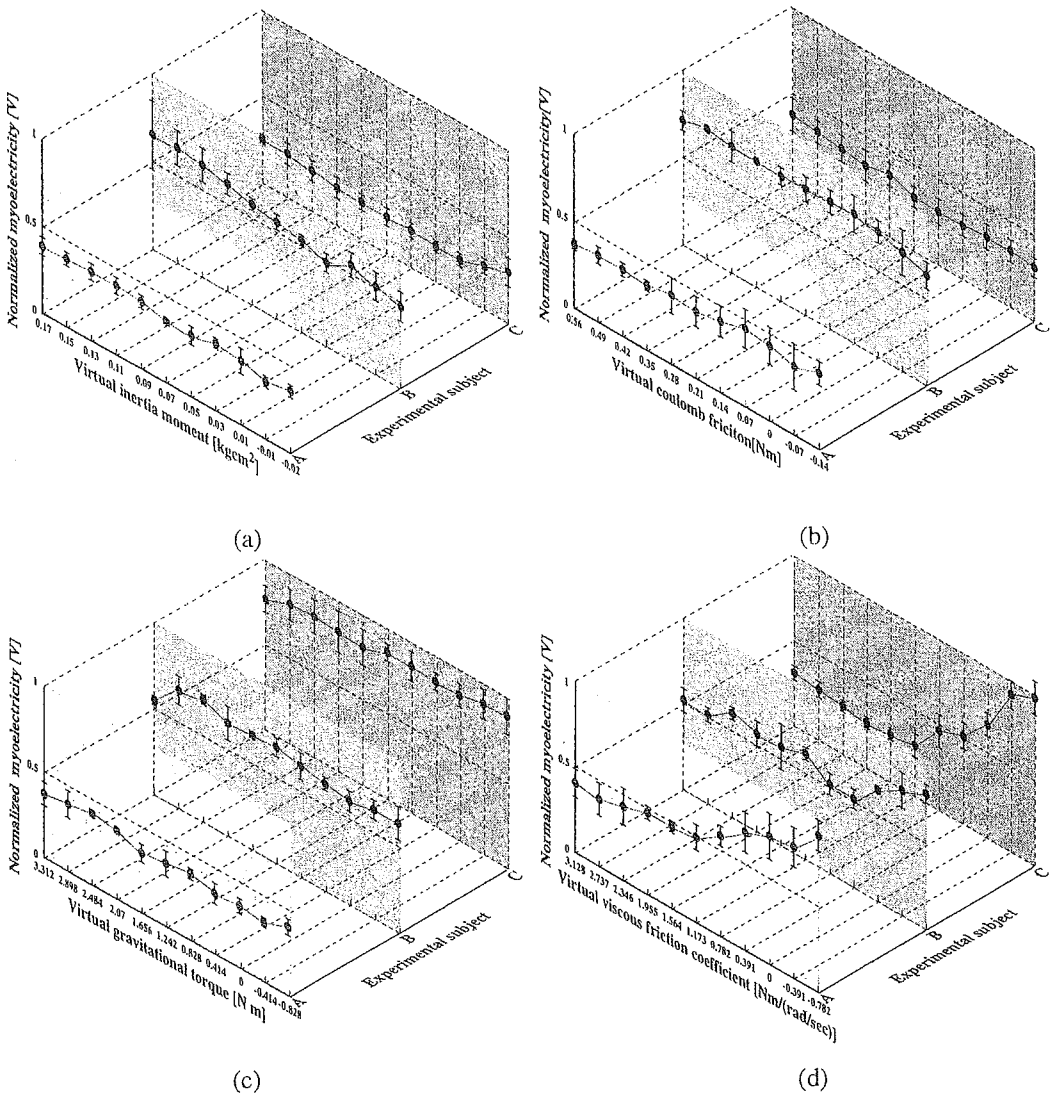

Fig. 7　Experimental results of myoelectricity at extensor muscle.

かった．仮想粘性摩擦に関しては仮想慣性モーメントの調整が影響すると考え，前章の実験と同様に条件を設定し，仮想粘性摩擦の変化と運動データの傾向に着目して再び結果を考察する事にした．

実験結果を図8に示す．(a)，(b)，(c) はそれぞれ被験者A，B，Cデータである．各データは上から負荷トルク，装着者の主観による評価，屈筋，伸筋の表面筋電位の順になっており，表面筋電位と負荷トルクに関しては薄い印で仮想粘性摩擦のみ補償した場合のデータを併記した．また負荷トルクの最小値が表れた仮想粘性摩擦係数ではデータに縦線を表示させた．

(a)，(b)，(c) の全体的な傾向としては，粘性摩擦のみ補償した実験結果と比べ負荷トルクと伸筋での表面筋電位が低下しており，屈筋の表面筋電位に関しても部分的に値が減少している．これにより，仮想クーロン摩擦の補償による直接的な負荷の軽減と共に，仮想慣性モーメントを0と設定する事で，仮想粘性摩擦の減少に伴って生じる慣性による負担も軽減されたと考えられる．しかし仮想粘性摩擦が比較的低い値で負荷トルクと表面筋電位が増加する傾向は依然と表れており，これによって慣性モーメントの補償とは関係無く，被験者は軽減された粘性摩擦に対応して自ら関節関節回りのインピーダンスを高めている可能性があると判断できる．

装着者の主観による評価では，仮想粘性摩擦の減少と共に操作感は悪化，抵抗感は減少する傾向を示した．ここで負荷トルクの最小値と主観による評価との対応関係を解析したところ，被験者B，Cに関しては負荷トルクの最小値で操作感および抵抗感が0近辺，つまりアクチュエータを取り外した状態で運動した感覚に近くなっているのに対し，被験者Aでは被験者B，Cに比べて，操作感は僅かに悪く（-1），抵抗感は僅か

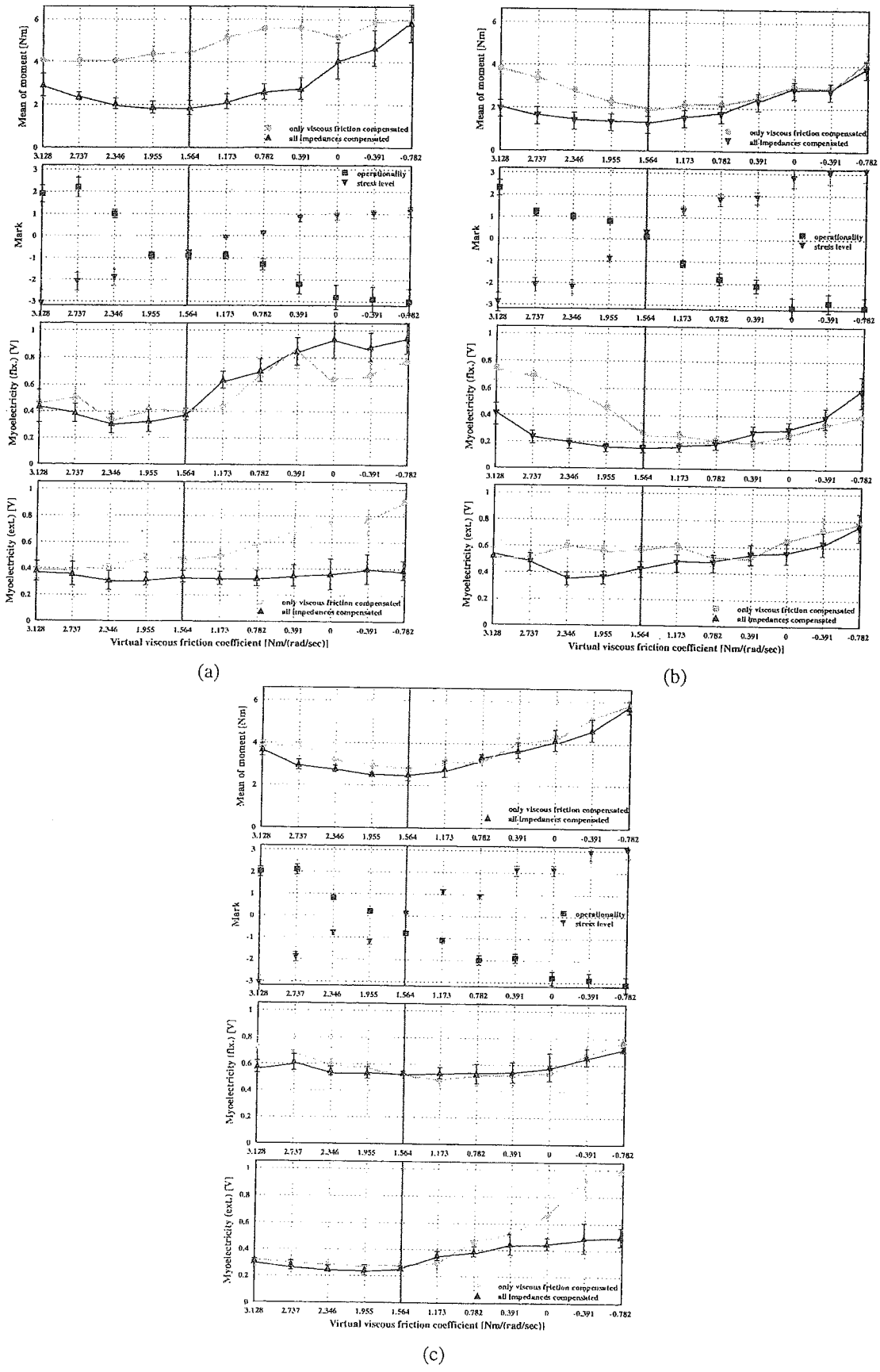

Fig. 8 Experiment for adjusting inertia moment, viscous friction, gravitational torque, coulomb friction

に重く（-1）表れた．しかし被験者A，B，Cに共通している特徴は，仮想粘性摩擦1.56[N·m/(rad/sec)]で負荷トルク最小値になっていることである．負荷トルクが最小になり，操作感と抵抗感が共に0である時の運動が最も理想的であると考えた場合，負荷トルクによる評価基準と被験者の主観による評価基準を同時に満たす為には仮想粘性摩擦1.56[N·m/(rad/sec)]を中心として仮想粘性摩擦を調整すればよいと考えられる．

従って，これらの実験結果をまとめると，振り運動における外骨格型パワーアシストシステムの各インピーダンスを設定する基準は，(1)仮想慣性モーメントと仮想クーロン摩擦は0に近い値に設定する事，(2)仮想重力モーメントは調整しない事，(3)仮想粘性摩擦は1.56[N·m/(rad/sec)]を中心として設定する事と決められる．

4. 考　　察

ここで被験者Aは被験者B，Cに比べ高い仮想粘性摩擦で負荷トルクの最小値が表れていることから，被験者Aは低い仮想粘性摩擦に対して被験者B，Cより敏感に関節回りのインピーダンスを高めている事が確認出来た．また被験者Aでは負荷トルクが最小になった仮想粘性摩擦で操作感は被験者B，Cと同様に表れたが，抵抗感は多少高く表れた．これらの原因として，同様の運動に対する被験者Aと被験者B，Cの感覚の違いや実験に対する熟達度の違いが考えられる．その後のアンケートの結果，被験者Aは過去10年間スポーツの経験が無く，被験者B，Cは最近までスポーツの経験がある被験者である事が分かった．直接的な原因であるかを明らかにする為に，今後スポーツの経験や運動神経の発達具合と関連させて検証する必要があると考えられる．

実験結果では仮想粘性摩擦補償による装着者の操作感改善は見られなかった．これによりHAL-3に現在採用しているアクチュエータの粘性摩擦は，負荷としての”抵抗感”に影響を与えているが，操作感を適度に高める効果もある事が分かった．

5. お　わ　り　に

本論文では装着型の下肢運動機能補助用パワーアシストシステムを用いて，振り運動でのインピーダンス基準設定方法を提案した．HAL-3を用いて外骨格系の仮想慣性モーメント，粘性摩擦等の仮想インピーダンス特性変化と装着者の操作感，負荷トルク及び筋の活動との関係を示し，これに基づき，外骨格系の影響を最小化した振り運動を実現する為の仮想インピーダンス調整基準を設定する事が出来た．今後，これらの結果を外骨格パワーアシストシステムの制御に適用する事で，歩行動作等振り運動が頻繁に行われる動作のパワーアシストを効率的に行う事が出来ると考えられる．

文　　献

(1) H. Kazerooni, S. L. Mahoney, “Dynamics and Control of Robotic Systems Worn by Humans” *Journal of Dynamic Systems, Measurement, and Control*, **vol. 113**, (1991-9), pp.379–387

(2) J. Rosen, M. Brand, M.B. Fushs, M. Arcan, “A Myosignal-Based Powered Exoskeleton System” *IEEE Transactions on Systems, Man, and Cybernetics-Part A: Systems and Humans* , **vol. 31**-No. 3, (2001-5), pp.210–222

(3) 木口　量夫，刈谷　臣吾，渡辺　桂吾，福田　敏男 “外骨格型ロボットによる人間動作補助の研究　（第2報，　複数のファジィ・ニューロ制御器を用いた人間肘運動補助用外骨格型ロボットの制御）” 日本機械学会論文集（C編），　**68**巻-668号, (2002-4), pp.　189–196

(4) 小菅一弘，藤澤佳生，福田　敏男 “仮想ツールダイナミクスに基づくマン・マシン系の制御” 日本機械学会論文集（C編），　**60**巻-572号, (1994-4), pp.　211–217

(5) 辻　敏夫, 加藤 荘志, 金子 真, “人間-ロボット系の追従制御特性”, 日本ロボット学会誌 , **Vol.18**-No. 2, (2000-3), pp. 285-291.

(6) 山田　陽滋，鴻巣　仁司，森園　哲也，梅谷　陽二 “自動車組立工程における搭載作業のためのスキルアシストの提案” 日本機械学会論文集（C編），　**68**巻-666号, (2002-2), pp. 509-516

(7) Harry Dankowicz, Jesper Adolfsson, Arne B. Nordmark, “Repetitive Gait of Passive Bipedal Mechanism in a Three-Dimensional Environment”, *Journal of Biomechanical Engineering, ASME* , **Vol.123**-No, (2001), pp. 40-46.

(8) 山本澄子，“第1部，第3章，　歩行時の関節モーメントと筋活動” 関節モーメントによる歩行分析，　医歯薬出版株式会社, (1999), pp. 19

(9) J. Okamura, H. Tanaka, Y. Sankai, “EMG-based Prototype Powered Assistive System for Walking Aid,” *Asian Symposium on Industrial Automation and Robotics (ASIAR’99)* , Bangkok, Thailand, pp.229–234, 1999.

(10) T. Nakai, S. Lee, H. Kawamoto, Y. Sankai, “Development of Power Assistive Leg for Walking Aid using myoelectricity and Linux,” *Asian Symposium Industrial Automation and Robotics*, (2001-6), pp.1295–1310.

(11) S. Lee, Y. Sankai, “Power Assist Control for Walking Aid with HAL-3 Based on EMG and Impedance Adjustment around Knee Joint” *Proc. of IEEE/RSJ International Conference on Intelligent Robots and Systems*, (2002-9), pp.1499–1504.

(12) S. Lee, Y. Sankai, “Natural Frequency-Based Power Assist Control for Lower Body with HAL-3” *Proc. of 2003 IEEE International Conference on Systems, Man, and Cybernetics*, (2003-10), pp. 1642–1647.

(13) 大谷 孝司, 柿崎 隆夫, 中川 三男, “多関節マニピュレータの動力学パラメータ同定に関する実験的検討”, 日本ロボット学会誌,　**11**巻-7号, (1993-10), pp. 1083-1092

(14) Mohamed Sahbi BEN-LAMINE, Satoru SHIBATA, Kanya TANAKA, Akira SHIMIZU "Impedance Characteristics of Robots Considering Human Emotions" *JSME International Journals* (*Series C*), **Vol.40**-No. 2, (1997), pp. 309-315

(15) H. I. Krebs, N. Hogan, M. L. Aisen, B. T. Volpe, "Robot-Aided Neurorehabilitaion" *IEEE Transactions on Rehabilitation Engineering*, **vol. 6**-No. 1, (1998-3), pp.75–86

2005 IEEE/RSJ International Conference on Intelligent Robots and Systems

(rking as Operator's Muscle using Biological and Dynamical Information

Tomohiro Hayashi, Hiroaki Kawamoto and Yoshiyuki Sankai
Graduate School of Systems and Information Engineering
University of Tsukuba
1-1-1 Tennodai, Tsukuba-shi Ibaraki-ken, Japan
iros@golem.kz.tsukuba.ac.jp

Abstract **- For assisting human motion, assistive devices working as muscles would be useful. A robot suit HAL (Hybrid Assistive Limb) has been developed as an assistive device for lower limbs. Human can appropriately produce muscle contraction torque and control joint viscoelasticity by muscle effort such as co-contraction. Thus, to implement functions equivalent to human muscles using HAL, it is necessary to control viscoelasticity of HAL as well as to produce torque in accordance with operator's intention. Therefore the purpose of this study is to propose a control method of HAL using Biological and Motion Information. In this method, HAL produces torque corresponding to muscle contraction torque by referring to the myoelectricity that is biological information to control operator's muscles. In addition, the viscoelasticities of HAL are adjusted in proportion to operator's viscoelasticity that is estimated from motion information by using an on-line parameter identification method. To evaluate the effectiveness of the proposed method, the method was applied to a swinging motion of a lower leg. When this method was applied, HAL could work like operator's muscles in the swinging motion, and as a consequence, the muscle activities of the operator were reduced. As a result of this experiment, we confirmed the effectiveness of the proposed method.**

Index Terms **- *robot suit, viscoelastic properties, impedance control, on-line parameter identification, myoelectricity.***

I. Introduction

Assistive devices that can work as motor organs would be useful for assisting or enhancing human motion. We have developed a robot suit HAL (Hybrid Assistive Limb) as an assistive device for operator's lower limb [1-3].

In order to use HAL as operator's muscles, HAL has to work as a torque generator like muscles. It is necessary that HAL detect operator's intention to produce muscle torque voluntarily, in order to produce torque. It is useful to use biological information such as myoelectricity to detect operator's intention [2, 4]. Additionally, the operator cannot only produce the muscle torque, but also control joint viscoelasticity by muscle effort such as co-contraction of the flexor and extensor [5, 6]. The joint stiffness is adjusted for different motions. When the operator needs a high joint viscoelasticity, it is useful to increase a viscoelasticity of an actuator of HAL for assistance. Hence, it is also necessary to control viscoelasticity of HAL adaptively by referring to operator's joint viscoelasticity. It is necessary to estimate operator's viscoelastic properties using motion information because it is difficult to measure them directly.

Therefore, the purpose of this study is to propose a control method of the robot suit using Biological and Motion Information to use the robot as operator's joint muscles.

In this paper, the proposed method is applied to HAL Mark three (HAL-3) [2, 3] in the case of swinging motion of the lower leg. Fig. 1 shows the configuration of HAL-3. It consists of exoskeleton frame with actuators for knee and hip joints in each leg. The angle of each joint is measured with a potentiometer attached to the joint. To prevent hyperextension or hyperflexion, every actuator is equipped with mechanical limiters.

II. Control Method of HAL by Referring to Operator's Biological and Motion Information

A. Actuator Control based on Biological Information

In this section, we describe a method to produce torque corresponding to muscle contraction torque by actuators of HAL using the myoelectricity.

To detect myoelectricity, two sensor units are attached on operator's skin near the flexor and the extensor driving the targeted joint as shown in Fig. 2. The sensor unit consists of two electrodes and an instrumentation amplifier. Two signals of myoelectricity from the flexor and extensor are filtered and amplified. The myoelectric activity $E(t)$, which is an amplitude envelope of myoelectricity, is defined as follows:

$$E(t) = \sqrt{(1/T)\int_{t-T}^{t} m^2(t)\,dt} \qquad (1)$$

where m is the measured myoelectricity. This equation is applied to both the flexor and extensor of the targeted joint. The myoelectric activity is calculated online.

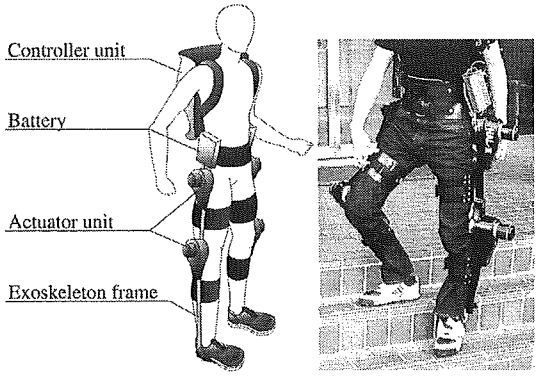

Fig. 1 Configuration of the robot suit HAL-3.

Then, the estimated muscle torque $\hat{\mu}$ is given by

$$\begin{aligned}\hat{\mu} &= \hat{\mu}_{ex} - \hat{\mu}_{flex} \\ &= (a_e E_e(t) + b_e) - (a_f E_f(t) + b_f)\end{aligned} \quad (2)$$

where $E_f(t)$ and $E_e(t)$ are the myoelectric activities of the flexor and extensor respectively, a_f, a_e, b_f and b_e are conversion coefficients from myoelectric activities to the contraction torque. By using estimated muscle torque, the torque τ_μ which HAL produces is given by

$$\tau_\mu = \alpha_\mu \hat{\mu} \quad (3)$$

where α_μ is a gain parameter.

A calibration exercise is necessary in order to obtain the conversion coefficients in (2). For the calibration, HAL has outputted steady torque pattern as a reference torque, and the operator putting on HAL has produced torque to compete against the reference torque without producing co-contraction as far as possible. The calibration exercise has been individually performed to the flexor and extensor of the joint. To obtain values of the conversion coefficients, a conventional least-square method has been applied. One of the results of the calibration exercise is shown in Fig. 3. The conversion coefficients apparently depend on operator's physical condition and the attached location of the sensor unit. Hence, the calibrating motion must be carried out, whenever the operator put on HAL.

B. Musculoskeletal Model of Operator's Lower Limb Working with HAL

We have constructed a musculoskeletal model of operator's lower limb equipped with the exoskeleton-actuator of HAL for estimating viscoelastic properties of operator's joint muscles and for controlling the properties of HAL.

In this study, muscles acting on a joint are regarded as one muscle group. Fig. 4 shows a model of muscle group around operator's knee joint as an example. The muscles in the group can respectively produce torque toward the contracting direction, but cannot produce it toward the extending direction. Thus, the muscle group needs two torque generators corresponding to the two directions.

Viscoelastic properties of the muscle group can be represented as a combination of a viscous element and an elastic element. We have assumed that the operator can modify the viscosity and elasticity with time. Hence, the two elements are defined as time-varying parameters.

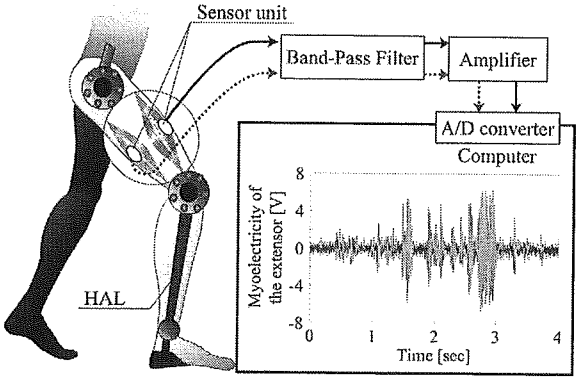

Fig. 2 Process of measuring myoelectricity.

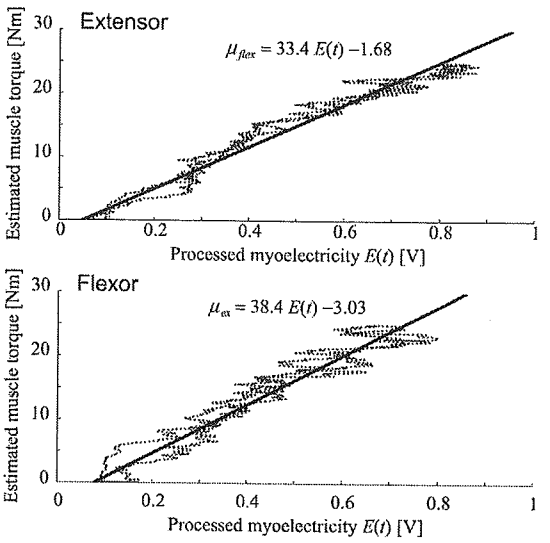

Fig. 3 One of the results of the calibration exercise.

Operator's leg with HAL is regarded as a multilink pendulum system to construct the musculoskeletal model. Fig. 5 shows the musculoskeletal model of operator's lower leg as an example. The motion equation of the i-th link of the model is expressed as follows:

$$I_i\ddot{\theta}_i + (D_i + R_i)\dot{\theta}_i + K_i\,\theta_i + M_i g l_i \sin\theta_i = \tau_i + \mu_i + \sigma_i \quad (4)$$

where θ is angle of a joint, I is total inertia around the joint, D and K are respectively the viscous and elastic coefficients of operator's muscle group, R is the viscous coefficients of the actuator of HAL, M is the mass of operator's leg link equipped with exoskeleton-actuator of HAL, g is the gravitational coefficient, l is the distance between the joint and the center of mass of operator's leg link with the exoskeleton, τ is torque produced by the actuator of HAL, μ is muscle torque produced by the operator, σ is the total interaction torque between adjacent links and suffix i is joint id. The parameters D and K are defined as time-depending parameters.

D. Method to Control Viscoelastic Properties of HAL

In this section we describe a method to control viscoelastic properties of HAL. In this study, actuator torque τ_ζ to control viscoelastic properties is determined based on impedance control method. τ_ζ of i-th joint is given by

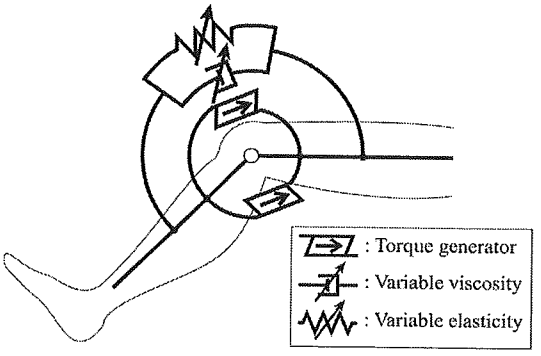

Fig. 4 Model of operator's muscle group around knee joint. Arrows in this figure mean contraction directions.

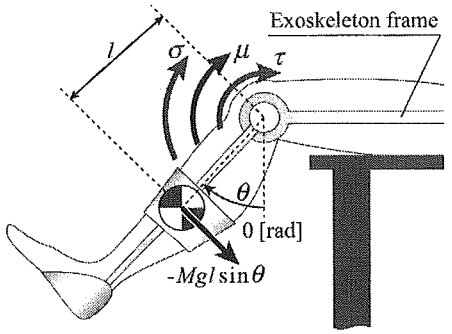

Fig. 5 Configuration of the musculoskeletal model of operator's lower leg equipped with HAL.

$$\tau_{i\zeta} = \alpha_{i\zeta}\left(-D_i\dot{\theta}_i - K_i\theta_i\right) \tag{5}$$

where $\alpha_{i\zeta}$ is a gain parameter.

In order that HAL works as muscles, the torque τ produced by its actuator is expressed as follows.

$$\tau_i = \tau_{i\zeta} + \tau_{i\mu} + \tau_{ic}. \tag{6}$$

where τ_{ic} is the torque to compensate mechanical impedance depending on exoskeleton-actuators of HAL [7, 8]. Although it is difficult to compensate all mechanical impedance of HAL absolutely, applying the compensation torque can sufficiently reduce the load derived from the impedance in actual use.

Substituting (6) into (4) gives

$$\begin{aligned}&(I_i - I_{ih})\ddot{\theta}_i + (1+\alpha_{i\zeta})D_i\dot{\theta}_i + (1+\alpha_{i\zeta})K_i\theta_i + M_i g l_i \sin\theta_i \\ &= (1+\alpha_{i\mu})\mu_i + \sigma_i.\end{aligned} \tag{7}$$

This equation suggests that HAL produces actuator torque as if it amplified operator's muscle torque and viscoelastic properties according to the gain parameters $\alpha_{i\mu}$ and $\alpha_{i\zeta}$. In consequence, the proposed method would reduce loads on operator's muscles.

C. Estimation of Viscoelastic Properties of Operator's Muscle

In this section, we describe a method to estimate viscoelastic properties of operator's muscle group in real time in order to control viscoelastic properties of HAL. We take operator's lower leg as an example to describe the method to estimate operator's viscoelastic properties.

To linearize (4), some parameters are defined as

$$\begin{aligned}D' &= D + R \\ K' &= K + G(\theta) \\ G(\theta) &= \begin{cases}(Mgl\sin\theta)/\theta & (\theta \neq 0) \\ Mgl & (\theta = 0).\end{cases}\end{aligned} \tag{8}$$

By regarding the sum of τ, μ and σ as the input of the lower leg system, we can express the state-space form of the system (1) as follows.

$$\begin{cases}\dfrac{d}{dt}\begin{pmatrix}x_1(t)\\x_2(t)\end{pmatrix} = \begin{pmatrix}0 & 1\\ -K'/I & -D'/I\end{pmatrix}\begin{pmatrix}x_1(t)\\x_2(t)\end{pmatrix} + \begin{pmatrix}0\\1/I\end{pmatrix}u(t) \\ \theta(t) = (1\ 0)\begin{pmatrix}x_1(t)\\x_2(t)\end{pmatrix}\end{cases} \tag{9}$$
$$u(t) = \tau(t) + \mu(t) + \sigma(t).$$

We applied the Delta-Operator δ to the discrete-time form for realizing high sampling rate. For the state-space form written as (9), the discrete-time form in is given by

$$\begin{cases}\delta\begin{pmatrix}x_1(k)\\x_2(k)\end{pmatrix} = \begin{pmatrix}0 & 1\\ -K'/I & -D'/I\end{pmatrix}\begin{pmatrix}x_1(k)\\x_2(k)\end{pmatrix} + \begin{pmatrix}T_d/(2I)\\(1-DT_d/(2I))/I\end{pmatrix}u(k) \\ \theta(k) = (1\ 0)\begin{pmatrix}x_1(k)\\x_2(k)\end{pmatrix}.\end{cases} \tag{10}$$

The solution of (10) for $\theta(k)$ gives

$$\begin{aligned}&\theta(k) = \boldsymbol{\varphi}^T(k)\,\mathbf{X}(k) \\ &\mathbf{X}(k) = [e_1 - D'/I \quad e_2 - K'/I \quad T_d/(2I) \quad 1/I] \\ &\boldsymbol{\varphi}(k) = [\delta\theta(k)/E(\delta) \quad \theta(k)/E(\delta) \quad \delta u(k)/E(\delta) \quad u(k)/E(\delta)]\end{aligned} \tag{11}$$

where $E(\delta)$ is a state variable. When $\hat{\mathbf{X}}(k)$ is defined as an estimated parameter vector, the prediction error $e(k)$ is given by

$$e(k) = \theta(k) - \hat{\theta}(k) = \theta(k) - \boldsymbol{\varphi}(k)\hat{\mathbf{X}}(k). \tag{12}$$

By using weighted least-squares method, the update formula of the estimated parameter vector to minimize $e(k)$ is derived as follows.

$$\begin{aligned}\hat{\mathbf{X}}(k+1) &= \hat{\mathbf{X}}(k) + \mathbf{P}(k)\boldsymbol{\varphi}(k+1)\frac{\theta(k+1) - \boldsymbol{\varphi}^T(k+1)\hat{\mathbf{X}}(k)}{\rho + \boldsymbol{\varphi}^T(k+1)\mathbf{P}(k)\boldsymbol{\varphi}(k+1)} \\ \mathbf{P}(k+1) &= \frac{\mathbf{P}(k) - \mathbf{P}(k)\boldsymbol{\varphi}(k+1)\boldsymbol{\varphi}^T(k+1)\mathbf{P}(k)}{\rho\{\rho + \boldsymbol{\varphi}^T(k+1)\mathbf{P}(k)\boldsymbol{\varphi}(k+1)\}} \\ \mathbf{P}(0) &= \beta\,\mathbf{I} \qquad (\beta > 0)\end{aligned} \tag{13}$$

where ρ is a forgetting factor ($0 << \rho < 1$) and $\mathbf{I}$ is the unit matrix of 4×4.

To obtain parameters of the viscoelasticity of the muscle group, we should identify invariant parameters M, g, l and R in (4) before the estimation of the parameters of viscoelasticity. If the operator does not activate his muscles, the motion of operator's lower leg equipped with HAL can be expressed as follows.

$$I\ddot{\theta} + (D+R)\dot{\theta} + Mgl\sin\theta = \tau. \tag{14}$$

Additionally, the link model of the exoskeleton frame for the lower leg with the actuator of HAL is expressed as follows.

$$I_h\ddot{\theta} + R\dot{\theta} + M_h g l_h \sin\theta = \tau \tag{15}$$

where I_h is inertia around exoskeleton-actuator of HAL, M_h is the mass of the exoskeleton with the actuator, and l_h is the distance between the knee joint and the center of mass of the exoskeleton-actuator. Parameters in (14) and (15) have been beforehand identified [7-9].

To control the viscoelastic properties of HAL according to (5), it is necessary to know the angular velocity of the joint. In this study, the state observer is adopted. Applying a state observer to (10) gives

$$\begin{aligned}\delta\begin{pmatrix}x_1(k)\\x_2(k)\end{pmatrix} &= \begin{pmatrix}0 & 1\\ -K'/I & -D'/I\end{pmatrix}\begin{pmatrix}x_1(k)\\x_2(k)\end{pmatrix} + \begin{pmatrix}T_d/(2I)\\(1-DT_d/(2I))/I\end{pmatrix}u(k) \\ &+ \begin{pmatrix}g_1(k)\\g_2(k)\end{pmatrix}\{\theta(k) - \hat{\theta}(k)\}\end{aligned} \tag{16}$$

where g_1 and g_2 are observer gains. These gains must be adjusted to keep stability of the state observer because the lower leg model shown in (4) is designed as a time-varying system. In addition, it is desirable that a time constant of the state observer remains smaller than the electromechanical delay [10] in order to ensure tracking performance of the

parameter estimation. We have, therefore, predefined the time constant of the state observer. Then, stable eigenvalues λ_1 and λ_2 for the observer have been defined for satisfying predefined time constant. Two observer gains have recursively been updated. The updating forms of observer gains are

$$g_1(k) = \lambda_1 - \lambda_2 - D'(k)/I(k)$$
$$g_2(k) = \lambda_1 \lambda_2 - g_1(k) D'(k)/I(k). \quad (17)$$

III. Experiments

To evaluating the proposed method, it was applied to a swinging motion of a lower leg. The operator putting on HAL sat on a chair that has enough height to prevent his foot from grounding. The operator swung his right lower leg up and down. The operator was asked not to actuate other joints except the right knee. We have assumed a combination of foot and lower leg as one link, because ankle joints have been locked. From the above conditions, σ in (4) can be ignored.

To evaluate effectiveness of the proposed method, two types of experiments were carried out. In the first experiment (Experiment 1,) no assisting method was applied. HAL produced only the torque τ_c in (6) compensating its mechanical impedance. In the second experiment (Experiment 2,) the proposed method was applied. Torque produced by the actuator of HAL in this experiment was calculated according to (6). The gain parameters α_μ and α_ζ in were defined as 1.0 and 0.5 respectively.

For the experiments, targeted frequency for the swinging motion was 0.5 Hz. Targeted maximum angles for the extending direction and the flexing direction were respectively 1.0 and -0.3 radians. However, the operator was not required to follow "exactly" the targeted angles. The operator could confirm angle of the joint by a computer display in real time. For the experiments, multiple rehearsals were carried out before each experiment. The operator rested sufficiently between trials to curb the influence of muscular fatigues on his motions and myoelectricity [11].

A strain of the exoskeleton frame was measured in order to evaluate force applied to operator's lower leg by HAL. The strain gauge was attached to the frame between the fastening equipment for the lower leg and the actuator of the knee joint as shown in Fig. 6. When operator's joint is fixed, the obtained signal is proportional to the actuator torque produced by HAL. In the swinging motion, the obtained signal is thought to include influences of dynamics of exoskeleton system of HAL. However, the influences of dynamics are thought to be enough smaller than the applied force by HAL. Therefore, in this paper, we assume that the obtained signal is proportional to the force applied to operator's leg by HAL. In all experiments, the strain gauge signal was not used at all for the control of HAL.

IV. Results

A. Experiment 1 (Without Any Assisting Method)

Fig. 7 shows a typical cycle of the swinging motion without applying any assistance by HAL. Fig. 7-A shows transitions of the angle of the knee joint. Increase of the angle corresponds to the extension of the knee joint, and decrease of the angle corresponds to the flexion of the joint. To compare experimental results, we have defined swing-up phase and swing-down phase. The swing-up phase is defined as the period in which the angle and angular velocity of the knee joint are positive. The swing-down phase is defined as the period in which the angle and the angular velocity of the joint are positive and negative respectively.

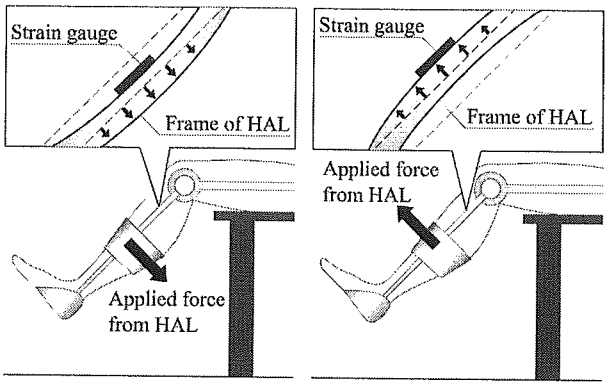

Fig. 6 Configuration to measure a strain of the exoskeleton-frame of HAL.

Fig. 7-B shows myoelectric activities. The myoelectric activity of the extensor has been plotted as positive, and that of the flexor has been plotted as negative. Myoelectric activities of the extensor and flexor were approximately 0.1 [V] and 0.04 [V] respectively, whenever operator's muscles around the knee joint were relaxed in all evaluation experiments. During swing-up phase, the myoelectric activity of the knee extensor was predominant and the direction of the muscle torque was the same as the rotating direction of the knee joint. This result suggests that the extensor worked as an agonist. During swing-down phase, the myoelectric activity of the extensor was predominant, suggesting that operator's muscle torque was found in the opposite direction of the rotation of the knee joint. In addition, simultaneous activation of both the extensor and flexor has been observed in swing-down phases, which suggests a co-contraction of the extensor and flexor.

Fig. 7-C shows the strain of the exoskeleton frame. The strain signal has been defined as positive values, when torque derived from HAL acts on operator's lower leg in the extending direction. During swing-up phases, the strain signal was found negative. Thus, the force applied to the lower leg from HAL worked in the flexural direction. During swing-down phase, the strain signal remained almost positive, which suggests that the force acted in the extending direction. Therefore, HAL, which has not produced assisting torque, is thought to have approximately acted in the direction opposite to the rotation of the knee joint.

B. Experiment 2 (Using the Proposed Method)

Fig. 8 shows a typical cycle of the swinging motion in which the proposed method was applied. For a comparison, the cycle of swinging motion without any assisting method is superposed here as dotted lines. Fig. 8-A shows the transition of the angle of the actuator of the knee joint.

Myoelectric activities around the knee joint are shown in Fig. 8-B. In this experiment, the myoelectric activity of the

extensor was smaller than the activity in the case of not applying assisting method. In addition, the co-contraction of the extensor and flexor has hardly been observed.

The strain of the exoskeleton frame is shown in Fig. 8-C. In swing-up phases, the strain signal was approximately positive. In addition, in the middle of swing-down phase, the strain signal increased. These results signify the force applied to the lower leg from HAL worked in the extending direction.

C. *Comparison of Experimental Results*

To confirm the effectiveness of the proposed method, in this section, we compare results of two experiments by focusing on the swing-up phase and swing-down phase. Fig. 9-A and Fig. 9-B show the mean values of the average myoelectric activities per each phase. The average myoelectric activities decreased when the proposed method was applied. On the other hand, average myoelectric activities of the flexor in swing-up phases were approximately 0.04 [V]. These results signify that the operator has not used the flexor and any assisting method had no effect on the flexor in swing-up phases. The average myoelectric activities of the flexor in swing-down phases were approximately 0.8 [V] through all experiments. This result signifies that the proposed method had little effect on the flexor during swing-down phases.

Fig. 9-C and Fig. 9-D show the mean values of the average strain gauge signals per each phase. The average strain signal was negative in swing-up phases without any assisting method. This result suggests that HAL acted on operator's knee joint in the flexing direction. In contrast, the average strain signals in swing-up phases were positive, when the proposed method was applied. These results suggest that HAL has effectively acted on operator's knee joint in the extending direction. Fig. 9-D suggests that HAL has most strongly acted on operator's knee joint in the extending direction during swing-down phases when the proposed method was applied.

V. Discussion

The swinging motion of the knee joint was carried out to confirm the effectiveness of the proposed method. In swing-up phases through the experiments, the extensor worked as the agonist and simultaneously the flexor was relaxed. Therefore we consider that the role of operator's muscles in swing-up phases was to produce the voluntary contraction torque to extend his knee joint. On the other hand, in swing-down phases, myoelectric activities of extensor were predominant. In addition, co-contractions of the extensor and flexor were observed, when the proposed method was not applied. Therefore, we consider that the major role of operator's muscles in swing-down phases was to restrain the flexion of his knee joint appropriately.

In Experiment I, The strain gauge signal was not zero

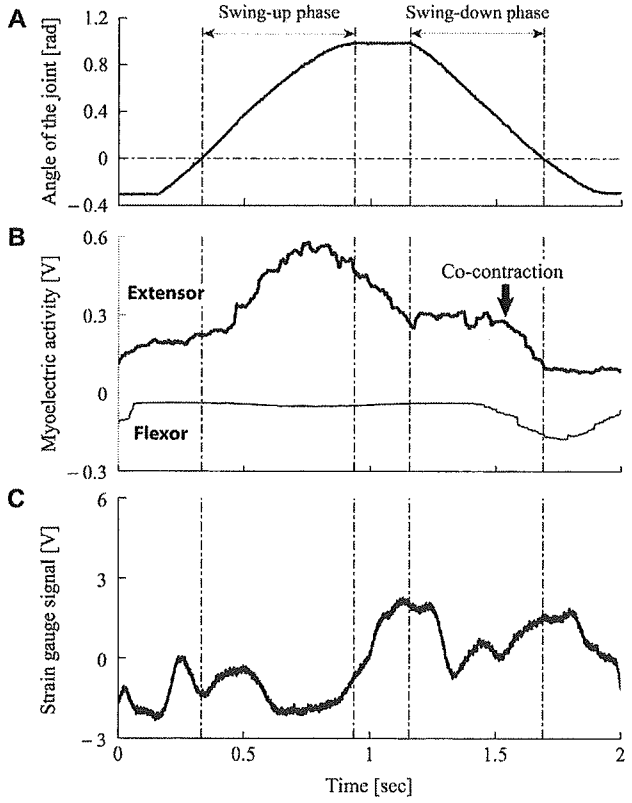

Fig. 7 A typical cycle of the swinging motion when no assisting method was applied

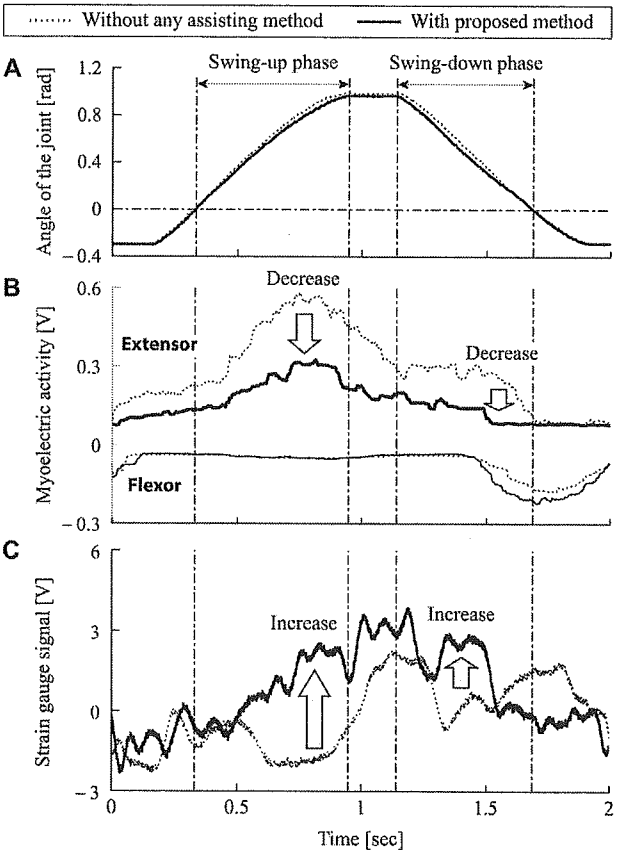

Fig. 8 A typical cycle of the swinging motion with applying the proposed method. Time-axis of this figure has been tuned so that the phase of the figure corresponds to those of Fig. 7.

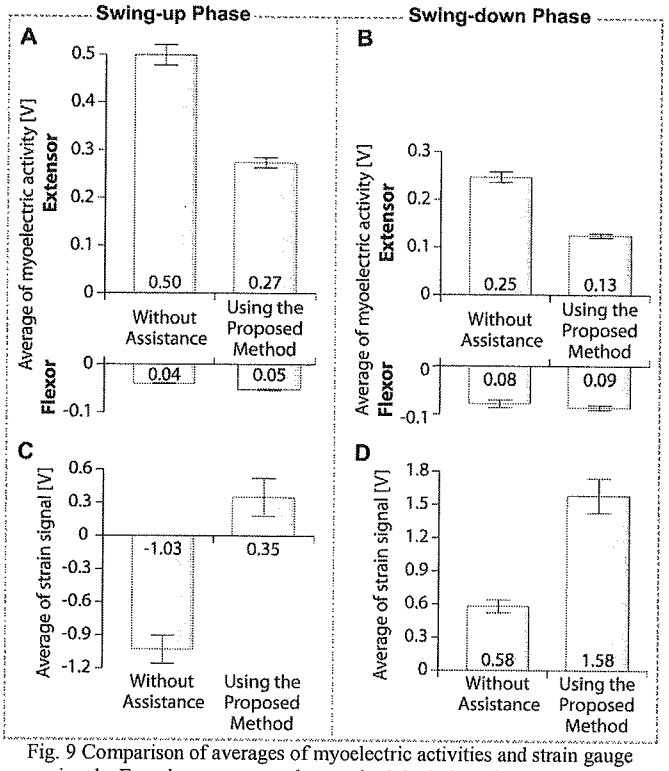

Fig. 9 Comparison of averages of myoelectric activities and strain gauge signals. Error bars represent the standard deviation of mean values.

although we compensated the mechanical impedance of HAL. It is very hard to completely compensate the mechanical impedance of practical exoskeleton-actuator system, because of an error of model parameters, a delay in control and so on.

When the proposed method was applied, HAL extended operator's knee joint in swing-up phases and acted on operator's knee joint in the extending direction in swing-down phases. These workings of HAL are fitting to major roles of operator's muscles in each phase. Additionally, reductions of operator's myoelectric activities were observed. Therefore, We consider that HAL has acted as muscles instead of operator's muscles appropriately by using the proposed method to control actuators of HAL.

However, when the proposed method was applied, the myoelectric activities of the flexor increased as compared to the case without any assisting method. This result implies also that the operator produced the muscle torque to flex the knee joint because HAL has restrained knee flexion more than the operator has expected. We consider that the gain parameter α_ζ =0.5 is still too large in this experiment. It will be necessary to develop a method to adjust the gain parameters appropriately as a future work.

VI. Conclusion

We have proposed the method to control actuators of HAL by referring to Biological and Motion Information to use the robot suit as operator's muscles. In this method, HAL produces torque corresponding to muscle contraction torque by referring to the myoelectricity that is the biological information to control operator's muscles. In addition, operator's viscoelasticities are estimated from motion information using an on-line parameter identification method. The model of operator's lower limb equipped with HAL was constructed in order to estimate operator's viscoelastic properties. The viscoelasticity of the actuator of HAL was adjusted to be proportional to operator's viscoelasticity by using the impedance control method.

To evaluate the effectiveness of the proposed method, the method was applied to a swinging motion of operator's lower leg. The experimental results suggested that the proposed method is useful to use HAL as operator's muscles. As a result of this experiment, we have confirmed the effectiveness of the proposed method.

Acknowledgment

This study was partially supported by the Ministry of Education, Culture, Sports, Science and Technology of Japan, Grant-in-Aid for Scientific Research (A).

References

[1] Okamura J., Tanaka H. and Sankai Y. EMG-based Prototype Powered Assistive system for Walking Aid. In Proc. Asian Symposium on Industrial Automation and Robotics (ASIAR'99), Bangkok, Thailand, pp.229-234, (1999).

[2] Nakai T., Lee S., Kawamoto H. and Sankai Y. Development of Power Assistive Leg for Walking Aid using EMG and Linux. In Proc. The 2nd Asian Conference on Industrial Automation Robotics (ASIAR2001), Bangkok, Thailand, pp.295-299, (2001).

[3] Kawamoto H. and Sankai Y. Power Assist System HAL-3 for Gait Disorder Person. In Proc. of International Conference on Computers Helping People with Special Needs (ICCHP 2002), Linz Austria, pp.196-203, (2002).

[4] Gordon K.E. and Ferris D.P. Proportional myoelectric control of a virtual object to investigate human efferent control. Experimental Brain Research, 159, pp.478-486.

[5] Winter D.A., Patla, A.E., Francois F., Ishac M. and Gielo-Perczak K. Stiffness Control of Balance in Quiet Standing. Journal of Neurophysiology 80, pp. 1211-1221, (1998).

[6] Gomi H. and Osu R. Task-Dependent Viscoelasticity of Human Multijoint Arm and Its Spatial Characteristics for Interaction with Environments. J Neurosci, 18, pp. 8965-78 (1998).

[7] Lee S. and Sankai Y. Power Assist Control for Walking Aid with HAL-3 Based on EMG and Impedance Adjustment around Knee Joint. In Proc. of IEEE/RSJ International Conf on Intelligent Robots and Systems (IROS 2002), EPFL, Switzerland, pp.1499-1504, (2002).

[8] Lee S. and Sankai Y. Power assist control for leg with hal-3 based on virtual torque and impedance adjustment. In Proc. IEEE International Conference on Systems, Man and Cybernetics (SMC), Hammamet, Tunisia, TP1B3 (CD-ROM), (2002).

[9] Lee S. and Sankai Y. The Natural Frequency-Based Power Assist Control for Lower Body with HAL-3. In Proc. of IEEE International Conference on System, Man and Cybernetics (SMC), Washington USA, (2003).

[10]Cavanagh, P.R., Komi, P.V. Electromechanical Delay in Human Skeletal Muscle under Concentric and Eccentric Contractions. European Journal of Applied Physiology, 42, 159-163 (1979).

[11]Park, E. and Meek, S.G. Fatigue compensation of the electromyographic signal for prosthetic control and force estimation. IEEE Transactions on Biomedical Engineering, vol. 40, Oct. (1993).

2005 IEEE International Workshop on Robots and Human Interactive Communication

Task Generation for Humanoid Robot Walking using Human Motion by Phase Sequence

Seong-Hoon Kim
Graduate school of Systems and Information engineering
University of Tsukuba
1-1-1, Tennoudai, Tsukuba, 305-8573,Japan
roman@golem.kz.tsukuba.ac.jp

Yoshiyuki Sankai
Graduate school of Systems and Information engineering
University of Tsukuba
1-1-1, Tennoudai, Tsukuba,305-8573, Japan
sankai@kz.tsukuba.ac.jp

Abstract **- The motion division, called "Phase", for generation "Task" of humanoid robot is effective method. Task could be realized by method for Phase transition, defined as "Phase Sequence", which can refer a skilled actual human motion without learning. In the method, guarantee for connection between the Phase transitions is important problem. This study aim to generate human mimicking Task for a humanoid robot based on an analysis of the human motion strategy with Phase Sequence method. In the approach, human motions were can be classified into several Phases based on the patterns of joint angle and floor reaction force. Injecting human motion data into a humanoid robot, we convert the joint angles into desired trajectories, which were transformed by the third-order Bezier curve and constraint function of configuration from actual motion., To realize, these methods, we did motion extraction experiment from human walking with capturing system. Furthermore, Phase transition method was applied by a given set of constraint conditions. As a result, Task was generated by simulator successfully. Then, walking Task for humanoid robot could be verified by proposed algorithm.**

Keywords – Humanoid robot, Phase, Phase Sequence, Walking Task, Human motion

I. INTRODUCTION

Humanoid robots would be suitable type for working in the human's space, but it did not have enough performance for adaptable motion in various environments so far. One primary reason for this is that multiple link structure of robots makes the motion generation be confused and ill-defined. Although human body has redundant structure, he/she can perform numerous motions well according to environments because the human's body is capable of managing to capricious conditions by acquired empirical skill innately. So it would be considered efficient to take advantage of this aspect for generating Tasks in various environments since the structure of a humanoid robot is similar to that of human's.

Some research of humanoid robotics adapting human motion has been presented for generating of numerous human-like patterns [1-4].

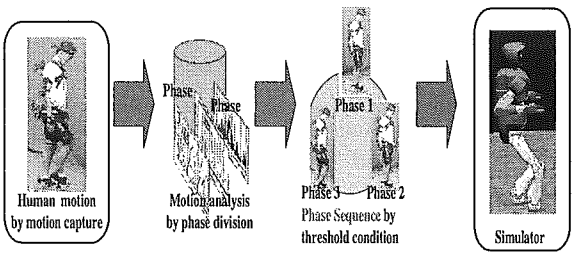

Fig.1 Overview of Task generation

These study has been excuted from viewpoint of demonstration of human gesture, observing and modifyng with learning algorithm. These study has been excuted from viewpoint of demonstration of human gesture, observing and modifyng with learning algorithm.

The feature of our approach is distinguished from above research. As a method for generating Task, we adopted method of Phase Sequence that can be assembled by Phase a meanning of divided motion unit. Furthermore, it would not require humanoid robot to observe human gesture and learning process from motion because skilled actual motion of human through experiment is applied.

In a previous study, we have explored by refering strategy of human motion for fundamental Task generation such as human care service and control on irregular terrain by Phase division [5-7].

This work was conducted as follows.

(1) Human's walking is measured with capturing and floor reaction force sensor system. Motion data, such as joint angle and floor reaction force, are acquired in this step.

(2) These motion were divided into several motion, called Phase, according to variation of acquired data. In this procedure, desired Task can be composed by several motion, which was accomplished and recomposed by linking Phases.

(3) The human motion can be classified as Phase with trajectories that were transformed adopting the three-

order Bezier curve, constraints function and contact condition in motion configurations via data of floor reaction force on the ground.

(4) To generate Task, the several Phases were transformed into a humanoid robot using trajectory planning and Phase Sequence, which has capable of transferring a part from its initial to desired position.

Figure 1 illustrates an overview of Task generation by proposed procedure.

In particular, our specific aims to expand a previous human mimicking Task generation algorithm based on human motion that has been analyzed using the continuing Phase Sequence method according to the predetermined order of events. When the Task is generated using the Phase Sequence method, each Phase transition operation should be capable of moving a part from its initial position to the desired position while simultaneously planning the motion trajectory. We introduce the Phase transition method based on threshold conditions from motion data, which is determined by the state of motion configuration in human. Therefore, if the individual Phase transition operation for sequence is appropriate, desired Task of a humanoid robot could be reproduced from the actual motion of human.

The reality of this approach and its applicability in a humanoid robot through motion capturing experiment were demonstrated by walking on regular surface.

II. ACQUIRING HUMAN MOTION DATA

Movement that can imply a change of place or position said in some way, to some kind, in all performance accomplished by human. Also, the degree to which movement is influenced by the structure of body. Every individual is taking a posture to determine suitable motion in environment. For analyzing motion strategies, we adopt a capturing system, which had used to measure movement with visual set. Side by side comparison of experiment with video snapshot is used to confirm correspondence between simulation and timing of real motion. Capturing and FRF(Floor Reaction Force) systems are shown in Figure 2. The description of this mechanism for measuring experiments presented in this chapter. And then the procedure to acquire data from human's actual motion will be described.

A. Measurement for Joint Angle

As the movement in one plane, the posture of body is at all times clearly determined by positional angles and displacement, which can be formed by the human's skeleton. Using a motion-capturing system, we can measure angle of human's walking posture. We used a mechanical capturing system that an actor puts on a mechanical suit in which many sensors are attached to the appropriate each joints to calculate the translation and rotation on the surface of whole body [8]. It is capable to capture 30~40 recording frames per a second Three dimensional posture of human's body are numerically determined from gyroscope at waist part, 44-potentialmeters mounted at each joints.

B. Implementation of the Floor Reaction Force

From the viewpoint of human's normal motion, the reaction force on floor, which occurs in the between foot and ground play important role in motion determination. If human's sole is contact with terrain or space, he/she tries to take a balance with some parts of body so as to avoid the stumble as quickly as possible. Therefore, we use FRF sensor in sole to acquire contact information on the ground as show in Figure 2(b).

III. ANALYSIS OF HUMAN MOTION

The humanoid robot consists of rigid links that are connected to several revolute joints, which permit relative motion of the neighboring link structure. Since, the type of performance by the form of contact with the ground, a transition movement in humanoid robot would be restricted within joint angle and kinematics parameter. However, it is difficult to define a motion patterns. Toward this problem, the method to define the humanoid robot motion based on analysis of human motion were considered. Such a technique also has the advantage to generating Task that adapt to environments or condition for a humanoid robot. The development method is described by the posture of actual humans.

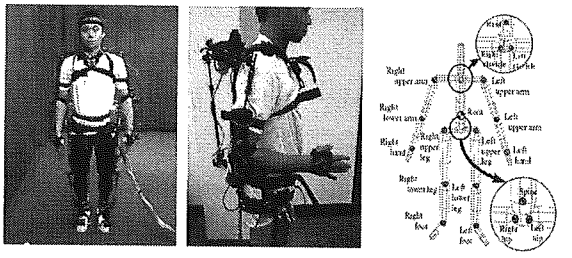

(a) Motion-capturing system

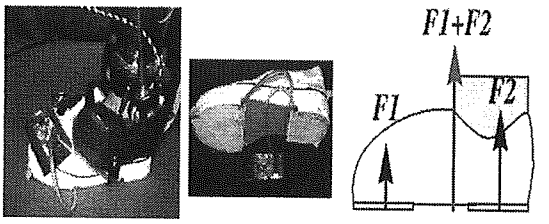

(b) Floor reaction force sensor

Fig. 2 Motion data acquisition system

A. Motion Division

A behavior of people indicates that there are an almost endless variety of means. In this paper, when the fundamental motion characteristics of all kinds are considered as shown in Figure 3.

Motions can be classified as essentially one or the other, or composition of the individuals. So the step in ours analysis, we divided into smaller fundamental motion called "Phase" according to investigation of turning point from extracted data. The individual Phases were linked to each other with order in order to generate the desired Task of humanoid robot. We define what this operation is "Phase Sequence"[9-10]. A motion composed of related Phases was define as "Task".

B. Walking Analysis

Normal human walking involves successive motion, which the body and lower-limbs are moved forward alternately. As the body weight moves forward, the upper end of the lower limb moves forward using the foot as an axis. The foot then swings forward to plan a new Phase. The end of the leg moves using the pelvis as an axis and the COG(Center of Gravity) also moves forward. As the stability of the body is disturbed, the limb continues to move forward, forming another.

The hip, knee, and ankle of each lower limb are included in a series of motion patterns, and these patterns are associated with stages of the rhythmic gait. Hence, the motion of each leg is divided into two categories: stance and swing. Figure 4 shows a snapshot of human walking motion based on data during Phase transition. We will use the notation "0", "SS", and "DS" to describe the stationary, single support, and double support periods, respectively.

-Phase 1 (0 - SS) describes the period of change beginning from a stationary posture to the start of the right leg swinging motion. The rear left sole FRF changes from b1 to b2 and the front left sole FRF increases from a1 to a2 because the COG starts to move gradually forward to the toe of left lower limb in preparation for the step. The right sole FRF decreases as the foot lifts off from the ground (a1' and b2'). In addition, the right joint angle is modified to the desired position (A1 -A2 and A1' - A2'). Since the lower limb starts to move forward, creating a new Phase in which the limb is in front of the forward-moving COG.

-Phase 2 (SS - DS) is the period of motion extending from the swinging of the right leg to supporting the upper body with both legs. In this Phase, the front left sole FRF decreases (a2 - a3) since the COG of the body has moved forward to the area above the supporting right foot.

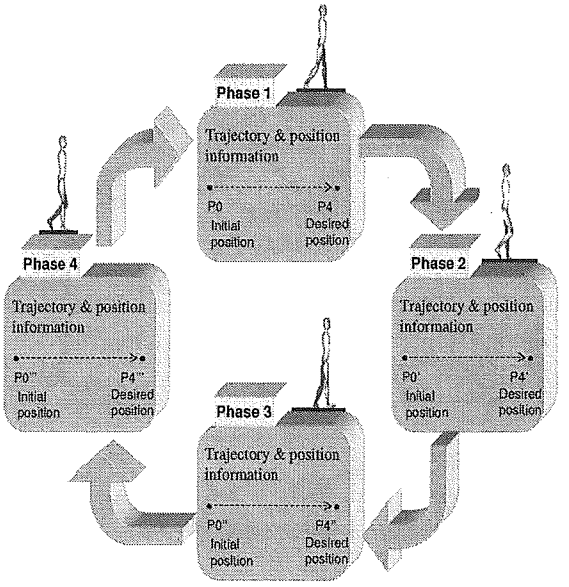

Fig.3.Example of performable walking Task by Phases Sequence

Accordingly, the front right sole FRF increases in gradual (a2' - a3'). The left lower limb is in contact with the ground until the COG of the body has moved forward, between A2 - A3 and A2' - A3'. In addition, the left lower limb is propelled forward to the desired position (B1' - B2' and B1 - B2).

-Phase 3 (DS - SS) can be defined the period that occurs between Phase 2 and the start of the left lower limb swinging motion, similar to Phase 1. The rear right sole FRF is not changes shown in b4' and b5' because of lifting-off right leg. The front right sole FRF changes from a4' to a5' because the COG moves toward the left lower limb and forward in preparation for the step. The left sole FRF starts to increase in preparation for lifting the foot off the ground. In addition, the angle of the joint changes (A3-A4 and A3'-A4') to the desired position.

-Phase 4 (SS - DS) is the final Phase in the walking motion. The COG moves forward in the manner described in Phase 2. The front right sole FRF increases (a5'- a6') when the heel of right leg is lifted off the ground, whereas the front left sole FRF decreases gradually (a5 - a6) as the forwarding upper body becomes supported on the lower limbs for stability. The angle of the left lower limb also increases (B3' - B4' and B3 - B4). The end of this Phase is the starting point for Phase 1.

In summary, Phases 1 and 3 are the periods when the upper body is supported by two legs, while Phases 2 and 4 occur while a leg is swinging and the body weight is exchanged between legs. From the FRF and joint angle data for the lower limbs, we know which sole is in contact with the ground and which one is swinging.